

Formation of helical domain walls in the fractional quantum Hall regime as a step toward realization of high-order non-Abelian excitations

Tailung Wu,^{1,2} Zhong Wan,¹ Aleksandr Kazakov,¹ Ying Wang,¹ George Simion,¹ Jingcheng Liang,¹ Kenneth W. West,³ Kirk Baldwin,³ Loren N. Pfeiffer,³ Yuli Lyanda-Geller,^{1,2} and Leonid P. Rokhinson^{1,2,4,*}

¹*Department of Physics and Astronomy, Purdue University, West Lafayette, Indiana 47907, USA*

²*Birk Nanotechnology Center, Purdue University, West Lafayette, Indiana 47907, USA*

³*Department of Electrical Engineering, Princeton University, Princeton, New Jersey 08540, USA*

⁴*Department of Electrical and Computer Engineering, Purdue University, West Lafayette, Indiana 47907, USA*



(Received 28 September 2017; revised manuscript received 22 February 2018; published 7 June 2018)

We propose an experimentally feasible platform to realize parafermions (high-order non-Abelian excitations) based on spin transitions in the fractional quantum Hall effect regime. As a proof of concept we demonstrate a local control of the spin transition at a filling factor $2/3$ and formation of a conducting fractional helical domain wall (fhDW) along a gate boundary. Coupled to an s -wave superconductor these fhDWs are expected to support parafermionic excitations. We present exact diagonalization numerical studies of fhDWs and show that they indeed possess electronic and magnetic structures needed for the formation of parafermions. A reconfigurable network of fhDWs will allow manipulation and braiding of parafermionic excitations in multigate devices.

DOI: [10.1103/PhysRevB.97.245304](https://doi.org/10.1103/PhysRevB.97.245304)

Topological quantum computation can be performed with Majorana fermions (MF) [1], but MF-based qubits are not computationally universal [2]. Parafermions (PFs), higher-order non-Abelian excitations, are predicted to have denser rotation group and their braiding enables two-qubit entangling gates [3,4]. A two-dimensional array of parafermions can serve as a building block for a system which supports Fibonacci anyons with universal braiding statistics [5], a holy grail of topological quantum computing. In an important conceptual paper Clark *et al.* proposed that PF excitations can emerge in the fractional quantum Hall effect (FQHE) regime if two counterpropagating fractional chiral edge states with opposite polarization are brought into close proximity in the presence of superconducting coupling [6]. Here we propose that domain walls formed at spin phase transitions in the FQHE regime have the prerequisite helical structure to support PF excitations when coupled to an s -wave superconductor. We demonstrate experimentally that in a triangular quantum well a 2D system can be tuned across a spin transition at a filling factor $\nu = 2/3$ using electrostatic gating. We also demonstrate formation of conducting channels at boundaries between incompressible polarized and unpolarized $\nu = 2/3$ states. These channels are formed from two counterpropagating $\nu = 1/3$ states with opposite spin orientation; we will refer to them below as fractional helical domain walls (fhDWs) in analogy to helical channels formed along the edges in the quantum spin Hall effect. Local control of polarization allows formation of a reconfigurable network of fhDWs with fractionalized charge excitations and, potentially, parafermion manipulation and braiding. We present exact diagonalization numerical studies of fhDWs.

Helical channels are commonly associated with the quantum spin Hall effect [7], topological insulators [8], or nanowires with spin-orbit interactions [9,10], where Coulomb interactions are not strong enough to fractionalize charges. A natural system to look for PFs is a 2D electron gas (2DEG) in the FQHE regime, where edge states support fractionally charged excitations. In the conventional QHE setting, though, edge modes are *chiral*. *Helical* channels can potentially emerge as domain walls during a quantum Hall ferromagnetic transition. It has been predicted that domain walls formed in the integer QHE regime at a filling factor $\nu = 1$ have helical magnetic order [11]. Experimentally, local electrostatic control of domain walls in the integer QHE regime at $\nu = 2$ was recently demonstrated in magnetic semiconductors [12], and their electronic and magnetic structure has been calculated [13].

In the FQHE regime spin transitions have been observed at a filling factor $\nu = 2/3$ and other fractions [14,15]. At the transition, the 2DEG spontaneously phase separates into regions of different spin polarizations, and conducting domain walls are formed along the domain boundaries [16,17]. An experimental challenge is to devise a system where spin transitions in the FQHE regime can be controlled locally, allowing formation and manipulation of DWs. Theoretically, neither magnetic nor electronic structure of these domain walls is known.

It has been realized that hard $\nu = 2/3$ edge states at the 2D gas boundaries are complex objects with chiral downstream propagation of charge excitations and neutral energy-carrying modes propagating both up- and downstream [18–20]. Recent experiments show that two copropagating $\nu = 1/3$ charge modes at the edge of a sample are weakly interacting and can be spatially separated [21]. Thus, a domain wall formed between two spin polarized domains at $\nu = 2/3$ ferromagnetic transition can be formally constructed from two counterpropagating

*Corresponding author: leonid@purdue.edu

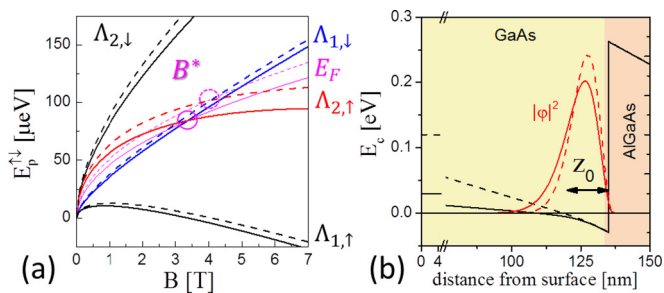


FIG. 1. (a) Energy spectrum of Λ levels for CFs, Eq. (1). For $\nu = 2/3$ (two filled Λ levels) the spin polarization of the top level changes at B^* , when $\Lambda_{1,\downarrow}$ and $\Lambda_{2,\uparrow}$ cross. Solid and dotted lines are calculated for two different values of the wave-function extent z_0 . (b) The calculated wave function in a triangular quantum well formed at a GaAs/AlGaAs heterojunction interface. Solid and dotted lines correspond to the two different gate voltages and show the change of z_0 . Note the break in the horizontal axis.

$\nu = 1/3$ chiral charge modes with opposite spin polarization, similar to the domain walls formation in the integer quantum Hall ferromagnetic transition [13].

Spin transitions in the FQHE regime can be readily understood within the framework of the theory of composite fermions (CFs) [22], where FQHE states at filling factors $\nu = \nu^*/(2\nu^* - 1)$ for $1/2 < \nu < 1$ are mapped onto integer QHE states with a filling factor ν^* for CFs. The energy spectrum of CF Λ levels with an index $p = 1, 2, 3 \dots$ can be written as

$$E_p^{\uparrow\downarrow} = \hbar\omega_c^{cf} \left(p - \frac{1}{2} \right) \pm g\mu_B B. \quad (1)$$

The CF cyclotron energy $\hbar\omega_c^{cf}$ is proportional to the charging energy $E_c = e^2/\sqrt{l_m^2 + z_0^2}$, where $l_m \propto \sqrt{B_\perp}$ is the magnetic length, $B_\perp = B \cos\theta$ is the out-of-plane component of the magnetic field B , and z_0 is the extent of the wave function in the out-of-plane direction. The second term is the Zeeman energy. Due to the difference in B dependencies of the two terms, levels $\Lambda_{p,\downarrow}$ and $\Lambda_{p+1,\uparrow}$ cross at some $B^* > 0$; see Fig. 1. Thus, for $\nu^* = 2$ (two Λ levels are filled) the top energy level undergoes a spin transition at B^* . The $\nu = 2/3$ state is unpolarized for $B < B^*$ and fully polarized for $B > B^*$.

Conventionally, FQHE spin transitions are studied in tilted magnetic fields, where *global* control of the field angle θ changes the ratio of Zeeman and cyclotron energies. For a triangular confinement, though, z_0 is gate dependent, $z_0 = z_0(V_g)$ [see Fig. 1(b)], and *local* control of E_c and B^* at a fixed B becomes possible. Within the Fang-Howard approximation of the wave function in a triangular well, $z_0 = 3/b$, where $b \propto n^{1/3}$ is a function of electron density. For GaAs parameters and $B^* \approx B_{\nu=2/3} \approx 4\text{--}6$ T, the field B^* becomes density and gate dependent: $\delta B^*/B^* \approx 0.3\delta n/n$, $\delta n/n = \delta V_g/V_g$. The field position of the $\nu = 2/3$ state is also density and gate dependent, $\delta B_{\nu=2/3}/B_{\nu=2/3} = \delta n/n$. Thus, for a well-developed wide $\nu = 2/3$ state and a sharp spin transition there should be a range of magnetic fields where spin polarization of the top level can be tuned locally by electrostatic gating.

In order to demonstrate electrostatic control of polarization we have grown a number of wafers where high mobility 2D electron gas is confined at a single GaAs/AlGaAs interface.

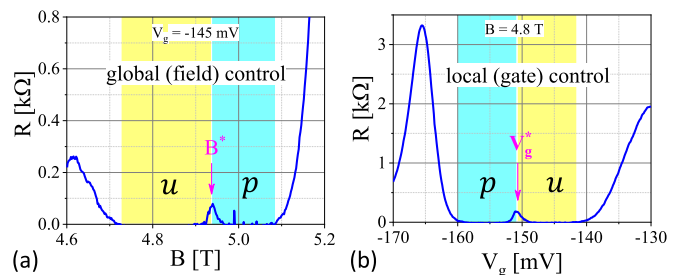


FIG. 2. Resistance in the vicinity of $\nu = 2/3$ state is measured as a function of (a) magnetic field B at a constant gate voltage V_g or (b) as a function of V_g at a constant B . Yellow and cyan colors mark unpolarized (u) and fully polarized (p) $\nu = 2/3$ states. B^* and V_g^* mark the spin transition.

Inverted GaAs/AlGaAs heterojunctions are grown by molecular beam epitaxy, the top layer is 130–230 nm thick GaAs, Si δ -doping placed 70–300 nm beneath the heterojunction interface. The top 25 nm of GaAs are lightly doped to reduce the surface pinning potential. In the main text we present data on devices fabricated from wafers A (Fig. 2) and D (Fig. 3), wafers parameters can be found in [23]. Inverted heterostructures allow electrostatic gating of a shallow 2D gas with no hysteresis, also in similar wafers proximity-induced superconductivity has been reported [24]. Ohmic contacts are formed by annealing Ni/AuGe/Ni/Au 6 nm/120 nm/20 nm/20 nm in a H_2/N_2 atmosphere. 10-nm-thick Ti gates are separated from GaAs and from each other by 50 nm Al_2O_3 grown by an atomic layer deposition (ALD). The gates are semitransparent and a 2D electron gas is created by shining red LED at ~ 4 K. Measurements were performed in a dilution refrigerator with the base temperature $T \approx 30$ mK using a standard lock-in technique with excitation current $I_{ac} = 0.1\text{--}10$ nA.

Magnetoresistance in the vicinity of a $\nu = 2/3$ plateau is shown in Fig. 2(a). At the base temperature a 0.35-T-wide incompressible state is interrupted by a small peak at $B^* = 4.94$ T. This peak has all the characteristics of a spin phase transition studied in the past, including strong current dependence and hysteresis with respect to the field sweep direction, which appears at high bias currents [15]. We identify this peak with the spin transition; unpolarized (u) and polarized (p) $\nu = 2/3$ states are highlighted with yellow and cyan on the plot. The most important data is shown in Fig. 2(b), where resistance is plotted as a function of a gate voltage V_g measured at a fixed magnetic field. Similarly to the field scan, an 18-mV-wide $\nu = 2/3$ plateau is interrupted by a small peak at $V_g^* = -151$ mV, which we identify with the spin transition. The transition peak is narrow, ≈ 6 mV with well-defined $\nu = 2/3$ states with different polarization on the two sides of the peak. Thus, it is possible to control spin polarization locally by electrostatic gating.

Formation of a conducting domain wall at a boundary between unpolarized and polarized $\nu = 2/3$ regions is shown in Fig. 3. A 2D gas is separated into two regions where density is independently controlled by gates G_1 and G_2 . The length of the gate boundary is 7 μm for the shown device. Resistances R_1 and R_2 for the 2D gases under the two gates are combined into a single plot in (c) in order to visualize

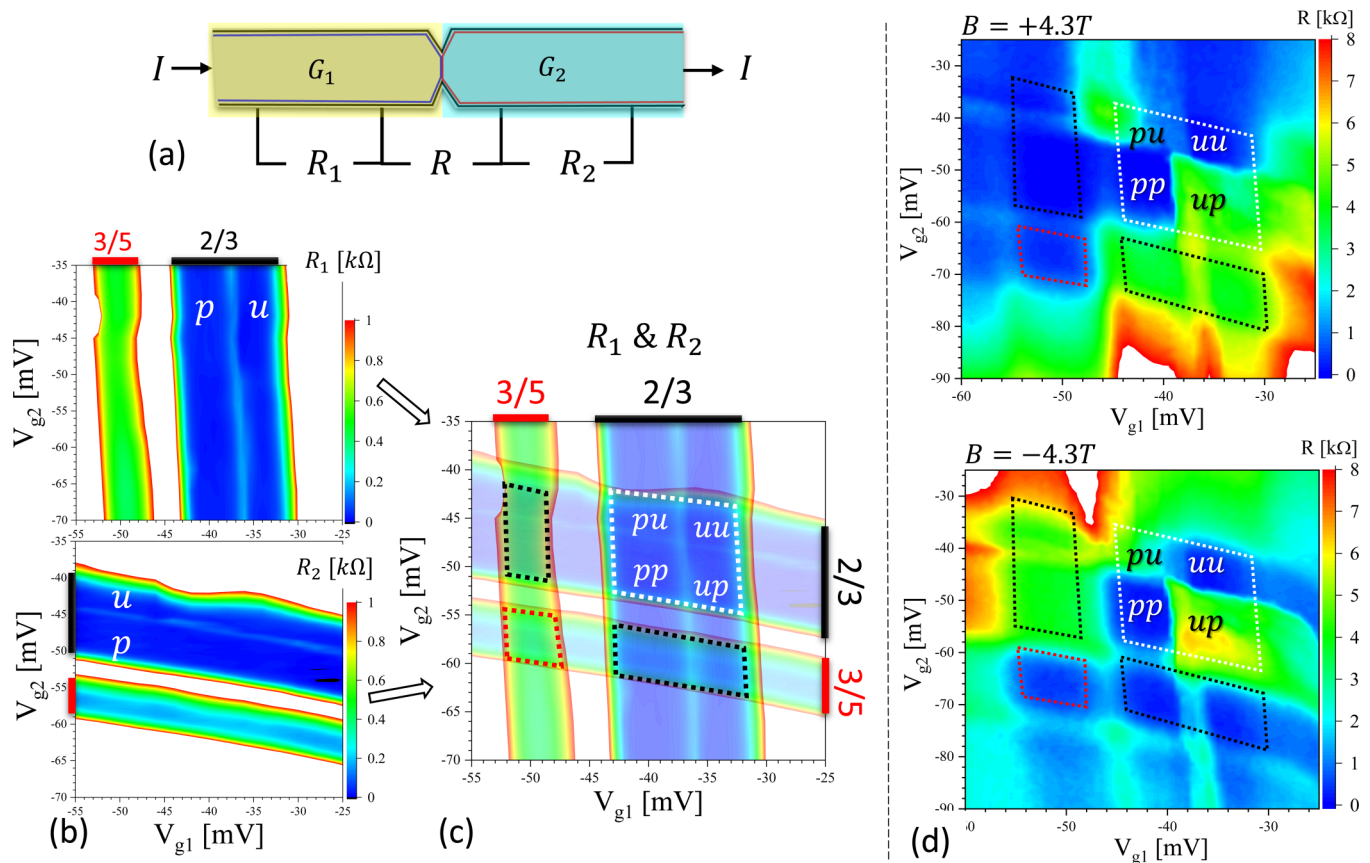


FIG. 3. (a) Sample layout. (b) Resistance R_1 and R_2 under gates G_1 and G_2 is measured as a function of gate voltages V_{g1} and V_{g2} . Letters u and p mark unpolarized and polarized states. In (c) R_1 and R_2 are plotted on top of each other. The region where $\nu = 2/3$ under both gates is outlined with a white dotted line, s_1s_2 indicates polarization under G_1 and G_2 . In (d) resistance R across the gate boundary is plotted for two fields directions. Nonzero R in (up) and (pu) quadrants indicates formation of a conducting domain wall between polarized and unpolarized $\nu = 2/3$ states. Lithographical length of the gate boundary is $7 \mu\text{m}$. Resistance in (b) and (c) is measured with $I_{ac} = 1.3 \text{ nA}$, in (d) with $I_{ac} = 0.13 \text{ nA}$.

regions in the $(V_{g1}-V_{g2})$ plane where FQHE states on both sites of the boundary overlap (a small coupling between the gates results in slightly nonorthogonal evolution of the features). A small bump in the middle of the $\nu = 2/3$ state is the spin transition (the data is taken with high $I_{ac} = 1.3 \text{ nA}$ in order for the transition to be visible above the noise level), and separates the $2/3$ region into four quadrants with different polarizations across the gate boundary. In (d) resistance measured across the gate boundary is plotted as a function of both gate voltages. In the region outlined red incompressible $3/5$ states are formed on both sites of the gate boundary and $R = 0$. A *chiral* channel is formed between $2/3$ and $3/5$ states (two regions outlined black). In this case resistance is gradient and field direction dependent: $R = 0$ or $R = 1/6R_q$, where $R_q = h/e^2$. Within the $2/3$ state $R = 0$ in the (pp) and (uu) quadrants, indicating formation of a well defined incompressible state under the gate boundary. When polarization of the $2/3$ state changes across the gate boundary R becomes nonzero indicating formation of a conducting channel. Resistance $R \sim 3\text{--}5 \text{ k}\Omega$ does not depend significantly on the direction of the density and polarization gradient (up or pu) nor on the magnetic field direction, consistent with the formation of a helical domain wall. In the current geometry resistance of the fhDW is not measured directly, within Landauer-Büttiker formalism we

extract $(10\text{--}20)R_q$ channel resistance for $2\text{--}7\text{-}\mu\text{m}$ -long fhDWs with no clear scaling with the length. The lack of scaling may indicate that scattering predominantly occurs in hot spots formed at trijunctions where fhDWs merge with edge states.

In order to investigate the structure of domain walls formed between spin-unpolarized and spin-polarized regions we performed exact diagonalization studies of a system with small number of particles. To simulate edge states we use the disk geometry [25,26] shown schematically in Fig. 4. Long-range Coulomb interactions between electrons are introduced using Haldane pseudopotentials. A neutralizing background and a confinement potential are used to hold electrons inside the disk. As is evident from experiments, the spin transition can be controlled by modulation of either Coulomb or Zeeman energies interchangeably; see, e.g., Fig. 2. In our modeling we use spatially dependent Zeeman effect to control spin polarization of the 2DEG. The central region of the disk of radius $R_1 = 2.9l_m$ is characterized by a high Zeeman energy term E_Z^{max} , while the outer region with the outer diameter $R_2 = 4.8l_m$ is set to $E_Z^{\text{min}} = 0$. The Zeeman term varies smoothly within $R_1 < r < R_1 + \Delta R$, where $\Delta R = 0.4l_m$, resulting in a smooth variation of wave functions across the disk and avoiding spurious effects originating from abrupt changes. Note that due to a strong penetration of electron wave functions

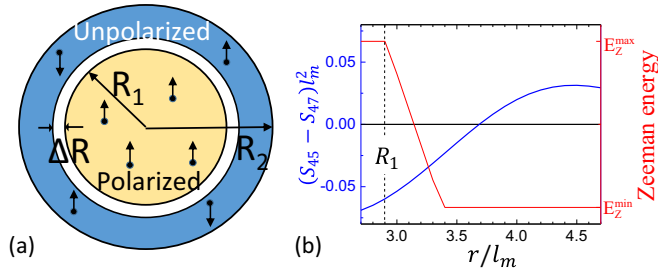


FIG. 4. (a) Disk geometry for the simulation domain. (b) The blue curve is the difference between spin densities $S_z(r)$ for the modes with angular momentum $L_z = 45$ and 47 , the current-carrying exciting states on the two sides of the domain wall formed around R_1 . Profile of the spatially dependent Zeeman interaction used to form the domain wall is shown in red.

from the $R_1 < r < R_2$ region into the $r < R_1$ region, the variation of the average spin splitting $\int \psi(r)^* E_z(r) \psi(r) d^2r$ for the two close modes on two sides of the domain wall is $<6\%$, similar to the experimental conditions. Therefore our model studies soft edges characterizing the experiment.

We include up to 12 electrons in the exact diagonalization calculation for fully spin-polarized states and eight electrons for unpolarized states or coexisting polarized and unpolarized states at $\nu = 2/3$. Energies and wave functions for the ground state and edge states, their density, and spin density distributions for the disk geometry have been calculated; see [23] for details. The ground state for eight particles has the total angular momentum projection $L_z = 46$, in agreement with the composite fermion theory [22]. The ground state is spin polarized in the interior part of the disk and spin unpolarized in the exterior area, as expected. The total spin projection of the ground state is $S_z = +2$. The lowest excited states with the same spin projection, which corresponds to the addition or subtraction of a single flux, has angular momenta $L_z = 45$ and 47 . These states are the current carrying states defining the domain wall. The difference in spin polarizations between these two states is shown in Fig. 4(b); it smoothly changes sign across the domain wall. There is $\approx 0.5l_m$ outward shift of the position of the midpoint of the domain wall in the actual spin-density profile relative to the profile of the defining

Zeeman term. This shift is due to smaller wave-function weights in the outward region.

The two edge states with different L_z on the disk have different angular velocities. When mapped onto a plane, these two states will have different linear velocities, i.e., their velocities will have counterpropagating components. Combined with the different spin polarization these states will have a finite overlap with Cooper pair wave functions in a proximity s -wave superconductor, as has been shown for domain walls in integer quantum Hall ferromagnets [13]. A proximity-induced topologically nontrivial superconductor, defined by the counterpropagating CFs modes with different polarization, is expected to emerge in the domain-wall region. Due to higher degeneracy of the composite fermion Λ levels compared to the degeneracy of the Landau levels, parafermion states will emerge at the boundary of topological and trivial s -wave superconductors, as predicted in Ref. [6].

In summary, we propose that domain walls formed during ferromagnetic spin transitions in the fractional quantum Hall effect regime can be used as building blocks to form topological superconductors that support parafermion excitations. Exact diagonalization study of spin transitions in a disk geometry confirms that domain walls, formed between spin-up and spin-down domains at $\nu = 2/3$, indeed possess electronic (two counterpropagating modes) and magnetic (opposite spin orientation for the two modes) structure needed to couple to an s -wave superconductor. We demonstrate that in triangular quantum wells spin transitions can be controlled locally by electrostatic gating and conducting helical domain walls can be formed in multigate devices. Such local control allows formation of reconfigurable networks of domain walls. In the presence of proximity-induced superconducting coupling the system becomes a reconfigurable network of one-dimensional topological superconductors with parafermion excitations.

Authors acknowledge support by the Department of Energy Awards No. DE-SC0008630 (T.W. and L.P.R.) and No. DE-SC0010544 (Y.L.-G. and J.L.), by Department of Defense Office of Naval Research Award No. N000141410339 (A.K., G.S., Y.L.-G., and L.P.R.), by National Science Foundation Grant No. DMR-1610139 (Z.W. and Y.W.), and by the Gordon and Betty Moore Foundation (K.W., K.B., and L.N.P.).

T.W., Z.W., and A.K. contributed equally to the experimental part of the work.

-
- [1] C. Nayak, S. H. Simon, A. Stern, M. Freedman, and S. D. Sarma, Non-abelian anyons and topological quantum computation, *Rev. Mod. Phys.* **80**, 1083 (2008).
- [2] M. Baraban, N. E. Bonesteel, and S. H. Simon, Resources required for topological quantum factoring, *Phys. Rev. A* **81**, 062317 (2010).
- [3] P. Fendley, Parafermionic edge zero modes in z_n -invariant spin chains, *J. Stat. Mech.* (2012) P11020.
- [4] J. Alicea and P. Fendley, Topological phases with parafermions: Theory and blueprints, *Annu. Rev. Condens. Matter Phys.* **7**, 119 (2016).
- [5] R. S. K. Mong, D. J. Clarke, J. Alicea, N. H. Lindner, P. Fendley, C. Nayak, Y. Oreg, A. Stern, E. Berg, K. Shtengel, and M. P. A. Fisher, Universal Topological Quantum Computation from a Superconductor-Abelian Quantum Hall Heterostructure, *Phys. Rev. X* **4**, 011036 (2014).
- [6] D. J. Clarke, J. Alicea, and K. Shtengel, Exotic non-Abelian anyons from conventional fractional quantum Hall states, *Nat. Commun.* **4**, 1348 (2012).
- [7] J. Maciejko, T. L. Hughes, and S.-C. Zhang, The quantum spin Hall effect, *Annu. Rev. Condens. Matter Phys.* **2**, 31 (2011).

- [8] M. Z. Hasan and J. E. Moore, Three-dimensional topological insulators, *Annu. Rev. Condens. Matter Phys.* **2**, 55 (2011).
- [9] R. M. Lutchyn, J. D. Sau, and S. D. Sarma, Majorana Fermions and a Topological Phase Transition in Semiconductor-Superconductor Heterostructures, *Phys. Rev. Lett.* **105**, 077001 (2010).
- [10] Y. Oreg, G. Refael, and F. von Oppen, Helical Liquids and Majorana Bound States in Quantum Wires, *Phys. Rev. Lett.* **105**, 177002 (2010).
- [11] V.I. Fal'ko and S.V. Iordanskii, Spin-Orbit Coupling Effect on Quantum Hall Ferromagnets with Vanishing Zeeman Energy, *Phys. Rev. Lett.* **84**, 127 (2000).
- [12] A. Kazakov, G. Simion, Y. Lyanda-Geller, V. Kolkovsky, Z. Adamus, G. Karczewski, T. Wojtowicz, and L. P. Rokhinson, Mesoscopic Transport in Electrostatically Defined Spin-Full Channels in Quantum Hall Ferromagnets, *Phys. Rev. Lett.* **119**, 046803 (2017).
- [13] G. Simion, A. Kazakov, L. P. Rokhinson, T. Wojtowicz, and Y. B. Lyanda-Geller, Impurity-generated non-Abelions, *Phys. Rev. B* **97**, 245107 (2018).
- [14] J. P. Eisenstein, H. L. Stormer, L. N. Pfeiffer, and K. W. West, Evidence for a spin transition in the $\nu = 2/3$ fractional quantum Hall effect, *Phys. Rev. B* **41**, 7910 (1990).
- [15] J. H. Smet, R. A. Deutschmann, W. Wegscheider, G. Abstreiter, and K. von Klitzing, Ising Ferromagnetism and Domain Morphology in the Fractional Quantum Hall Regime, *Phys. Rev. Lett.* **86**, 2412 (2001).
- [16] B. Verdene, J. Martin, G. Gamez, J. Smet, K. von Klitzing, D. Mahalu, D. Schuh, G. Abstreiter, and A. Yacoby, Microscopic manifestation of the spin phase transition at filling factor $2/3$, *Nat. Phys.* **3**, 392 (2007).
- [17] J. Hayakawa, K. Muraki, and Go Yusa, Real-space imaging of fractional quantum Hall liquids, *Nat. Nanotechnol.* **8**, 31 (2012).
- [18] C. L. Kane, M. P. A. Fisher, and J. Polchinski, Randomness at the Edge: Theory of Quantum Hall Transport at Filling $\nu = 2/3$, *Phys. Rev. Lett.* **72**, 4129 (1994).
- [19] A. Bid, N. Ofek, H. Inoue, M. Heiblum, C. L. Kane, V. Umansky, and D. Mahalu, Observation of neutral modes in the fractional quantum Hall regime, *Nature (London)* **466**, 585 (2010).
- [20] V. Venkatachalam, S. Hart, L. Pfeiffer, K. West, and A. Yacoby, Local thermometry of neutral modes on the quantum hall edge, *Nat. Phys.* **8**, 676 (2012).
- [21] R. Sabo, I. Gurman, A. Rosenblatt, F. Lafont, D. Banitt, J. Park, M. Heiblum, Y. Gefen, V. Umansky, and D. Mahalu, Edge reconstruction in fractional quantum Hall states, *Nat. Phys.* **13**, 491 (2017).
- [22] J. K. Jain, *Composite fermions* (Cambridge University Press, Cambridge, England, 2007).
- [23] See Supplemental Material at <http://link.aps.org/supplemental/10.1103/PhysRevB.97.245304> for the list of materials and theory details. See Refs. [27–36].
- [24] Z. Wan, A. Kazakov, M. J. Manfra, L. N. Pfeiffer, K. W. West, and L. P. Rokhinson, Induced superconductivity in high-mobility two-dimensional electron gas in gallium arsenide heterostructures, *Nat. Commun.* **6**, 7426 (2015).
- [25] Z.-X. Hu, E. H. Rezayi, X. Wan, and K. Yang, Edge-mode velocities and thermal coherence of quantum Hall interferometers, *Phys. Rev. B* **80**, 235330 (2009).
- [26] A. Tylan-Tyler and Y. B. Lyanda-Geller, In-plane electric fields and the $\nu = 5/2$ fractional quantum Hall effect in disk geometry, *Phys. Rev. B* **95**, 121302 (2017).
- [27] G. Giuliani and G. Vignale, *Quantum Theory of the Electron Liquid* (Cambridge University Press, Cambridge, England, 2005).
- [28] A. H. MacDonald, Edge States in the Fractional-Quantum-Hall-Effect Regime, *Phys. Rev. Lett.* **64**, 220 (1990).
- [29] C. W. J. Beenakker, Edge Channels for the Fractional Quantum Hall Effect, *Phys. Rev. Lett.* **64**, 216 (1990).
- [30] X. G. Wen and A. Zee, Topological structures, universality classes, and statistics screening in the anyon superfluid, *Phys. Rev. B* **44**, 274 (1991).
- [31] C. de C. Chamon and X. G. Wen, Sharp and smooth boundaries of quantum Hall liquids, *Phys. Rev. B* **49**, 8227 (1994).
- [32] Y.-H. Wu, G. J. Sreejith, and J. K. Jain, Microscopic study of edge excitations of spin-polarized and spin-unpolarized $\nu = 2/3$ fractional quantum Hall effect, *Phys. Rev. B* **86**, 115127 (2012).
- [33] D. B. Chklovskii, Structure of fractional edge states: A composite-fermion approach, *Phys. Rev. B* **51**, 9895 (1995).
- [34] I. A. McDonald and F. D. M. Haldane, Topological phase transition in the $\nu = 2/3$ quantum Hall effect, *Phys. Rev. B* **53**, 15845 (1996).
- [35] J. E. Moore and F. D. M. Haldane, Edge excitations of the $\nu = 2/3$ spin-singlet quantum Hall state, *Phys. Rev. B* **55**, 7818 (1997).
- [36] F. D. M. Haldane, Fractional Quantization of the Hall Effect: A Hierarchy of Incompressible Quantum Fluid States, *Phys. Rev. Lett.* **51**, 605 (1983).